LANGMUIR

pubs.acs.org/Langmuir Article

Segregation of Amine Oxide Surfactants in PVA Films

Rebecca J. Fong, Ophélie Squillace, Carl D. Reynolds, Joshaniel F. K. Cooper, Robert M. Dalgliesh, James Tellam, Florence Courchay, and Richard L. Thompson*

Cite This: *Langmuir* 2020, 36, 4795−4807 Read Online

ACCESS | Metrics & More | Article Recommendations | Supporting Information

ABSTRACT: The vertical depth distributions of amine oxide surfactants, *N*,*N*-dimethyldodecyl amine *N*-oxide (DDAO) and *N*,*N*-dimethyltetradecyl amine *N*-oxide (DTAO), in poly(vinyl alcohol) (PVA) films were explored using neutron reflectometry (NR). In both binary and plasticized films, the two deuterated surfactants formed a single monolayer on the film surface with the remaining surfactant homogeneously distributed throughout the bulk of the film. Small-angle neutron scattering and mechanical testing revealed that these surfactants acted like plasticizers in the bulk, occupying the amorphous regions of PVA and reducing its glass-transition temperature. NR revealed little impact of plasticizer (glycerol) incorporation on the behavior of these surfactants in PVA. The surfactant molecular area in the segregated monolayer was smaller for DTAO than for DDAO, indicating that the larger molecule was more densely packed at the surface. Surface tension was used to assess the solution behavior of these surfactants and the effect of glycerol incorporation. Determination of molecular area of each surfactant on the solution surface revealed that the structures of the surface monolayers are remarkably consistent when water is placed by the solid PVA. Incorporation of glycerol caused a decrease of molecular area for DDAO and increase in molecular area for DTAO both in solution and in PVA. This suggests that the head group interactions, which normally limit the minimum area per adsorbed molecule, are modified by the length of the alkyl tail.

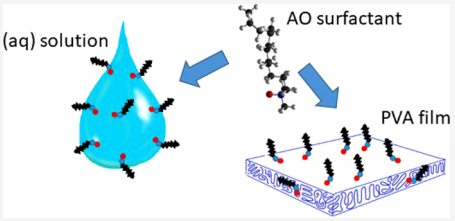

INTRODUCTION

Surface activity, which is the defining property of a surfactant, depends not only on surfactant molecular structure but also on its relationship with the medium in which it is dispersed. It is interesting therefore to consider whether an aqueous surfactant has recognizably similar behavior when water is replaced with a polar polymer as the "solvent". Although the behavior of surfactants in aqueous solution has been thoroughly explored, the case where the solution is replaced by a solid polymer has been addressed very little. The segregation of components in polymer films affects a wide range of industries and surfactant segregation has been shown to be important in the formation and properties of latices.[1−10]

In particular, poly(vinyl alcohol) (PVA) films encounter surfactant-rich environments in a number of areas, including as their use for the encapsulation of detergents for soluble unit dose laundry and dishwashing applications. The segregation and migration of surfactants at interfaces has potential implications in the film behavior and aging, impacting product performance and lifetime.

Poly(vinyl alcohol) is a water-soluble, synthetic, semicrystalline polymer with excellent film forming capability, good mechanical properties, and optical transparency.[11] Its application in food packaging makes use of the excellent barrier properties of PVA,[12] but PVA is additionally valued for its solubility, nontoxicity, and biodegradability[13,14] which contribute to its low overall environmental impact. These properties, alongside its resistance to organic solvents, have led to its increased use in the laundry industry as a film for packaging unit dose detergents.

PVA is prepared from the hydrolysis of poly(vinyl acetate) (PVAc). The characteristics of PVA are therefore dependent on its degree of polymerization (DP) as well as its degree of hydrolysis (DH), which dictates the number of hydroxyl groups present on the backbone, and must be controlled to optimize the polymer properties for its applications. PVA generally requires the addition of plasticizers to obtain the desired properties for many applications. Plasticizers are involatile, low molecular weight molecules that can modify the polymer matrix, increasing free volume and chain mobility. They are incorporated into materials in order to improve processability and flexibility, while maintaining desirable mechanical properties. Glycerol is one such compatible plasticizer for PVA.[15]

We have studied the segregation of a number of surfactants in poly(vinyl alcohol) (PVA) and a rich and diverse range of segregation behaviors have been observed in plasticized and nonplasticized films.[16,17] Plasticizer incorporation was also shown to significantly affect surfactant distribution; although

Received: January 13, 2020
Revised: April 8, 2020
Published: April 9, 2020

glycerol suppressed the surface activity of a nonionic surfactant in PVA, the opposite trend was seen for the cationic surfactant CTAB and the anionic surfactant sodium dodecyl sulfate (SDS). There are number of driving forces for this segregation that have been considered. First, it is expected that the component with the lowest surface energy will be enriched on the surface. Incompatibility between components can significantly increase surface segregation and lead to the formation of wetting layers. This is complicated, however, by the presence of multiple film components, including amphiphilic molecules.

Here, we study the segregation behavior of zwitterionic surfactants in order to identify factors affecting surfactant segregation in PVA. For the first time, we address the impact of surfactant tail length on distribution in films and furthermore explore the link between bulk film properties and surface segregation. Amine oxides are particularly interesting because of their small but highly polar head group (Figure 1).

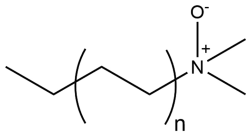

Figure 1. Structure of the amine oxide surfactants. For DDAO and DTAO, n is 5 and 6, respectively.

Compared to other surfactants of the same chain length, they are more hydrophilic, due to the unusually high dipole moment of the NO group.[18] An important feature of these surfactants is that the dipolar surfactant can be protonated at the oxygen and so therefore exists either as a nonionic or cationic species, depending on the pH of the solution.[19] We have used neutron reflectometry (NR) with deuterium labeling to identify surfactant segregation in spin-cast PVA films, and have used surface tension to compare the surface adsorption in solution with that identified in the solid polymer, aiming to address the question of how surfactant distribution in spin-cast films is related to behavior in solution. We also consider the more complex plasticized system in order to gain insight into interactions between films components and their compatibility. Furthermore, by extending this investigation to surfactant structuring in bulk, solution-cast films, we are able to study systems that are particularly relevant for soluble unit-dose technologies, an area of wide interest.

EXPERIMENTAL SECTION

Materials and Sample Preparation. PVA (Sigma-Aldrich P8136, M_w = 30−70 kg mol^{-1}, DH = 87−90%), glycerol (Sigma-Aldrich), *N*,*N*-dimethyldodecylamine *N*-oxide (DDAO; Sigma-Aldrich), *N*,*N*-dimethyltetradecylamine *N*-oxide (DTAO; Sigma-Aldrich), and d_5-glycerol (CK isotopes) were purchased and used as received. Deuterated DDAO (d_{25}) and DTAO (d_{29}) were synthesized at the Rutherford Appleton Laboratories.

PVA was dissolved in deionized water by heating to 75 °C with stirring to create 4 w/w % solutions. Similar aqueous solutions of other components (glycerol, d_5-glycerol, *h*-DDAO, *h*-DTAO, d_{25}-DDAO, and d_{29}-DTAO) were also made at 4% (w/w). Final 4% (w/w) solutions containing the desired proportion of the polymer with surfactant and/or glycerol were prepared by mixing the relevant solutions. These solutions were spin-cast into films of 40−100 nm, varying with surfactant and glycerol content by using a rotational speed of 3500 rpm during the drying stage. For neutron reflectivity and atomic force microscopy (AFM), solutions were spin-cast onto 55 mm diameter, 5 mm thick silicon blocks that has been first cleaned using permanganic acid, and subsequently acetone to remove traces of hydrophobic impurities in order to ensure film consistency. For small angle neutron scattering (SANS) and dynamic mechanical analysis (DMA), films were solution cast at 40 °C (rather than spin-cast) to give films of approximately 70 μm thick.

Neutron Reflectivity. The CRISP reflectometer at the Rutherford Appleton Laboratories was utilized to obtain vertical concentration versus depth profiles of spin-cast films under atmospheric conditions. Deuterium labeling provided contrast via the difference in scattering length density (SLD) of the components. The SLDs of the materials used are presented in Table 1. A complete reflectivity profile, from

Table 1. Scattering Length Densities of the Deuterated and Hydrogenous Film Components

component	SLD/10^{-6} Å^{-2}
PVA (88% DH)	0.75
Si	2.07
SiO_x	3.47
h-glycerol	0.61
d_5-glycerol	4.91
hDDAO	−0.20
d_{25}-DDAO	6.90
hDTAO	−0.21
d_{29}-DTAO	6.70

critical edge to background, was collected using three incident angles (0.25°, 0.6°, and 1.5°) in order to obtain a momentum transfer (Q) range of 0.008 < Q/Å^{-1} < 0.47. This required an acquisition time of 2 h per sample. Data were fitted using the Motofit package on IGOR.[20]

Surface Tensiometry. The surface tensions of dilute aqueous solutions of amine oxide surfactants and glycerol were measured using a KRÜSS K10 tensiometer, equipped with a Du Noüy ring. The platinum ring was cleaned by holding it in a microburner gas flame immediately before each measurement. Solutions were prepared using ultrahigh purity water, with a resistivity of 19.2 MΩ cm obtained from a Sartorius Arium R comfort water purification system. Surface tension measurements were performed at 20 °C. Repeat measurements were taken to check the reproducibility, and the accuracy of the measurements taken was ±0.1 mN m^{-1}.

Determination of Phase Diagrams. Dilute solutions (∼0.4 g) were prepared at defined ratios of PVA and DDAO/DTAO, in which the initial solute concentration was typically 10% (w/w). These solutions were applied to a glass slide, which was thermostated to 40 °C. The mass of the solution was regularly monitored, and the point at which the solution became cloudy was determined by visual inspection.

Small Angle Neutron Scattering. SANS measurements were carried out on solution-cast films, approximately 70 μm thick. The Larmor instrument at ISIS was used with a incident beam, yielding a fixed momentum transfer range of approximately 0.003 < Q < 0.7 Å^{-1}. Scattering was recorded as 2D detector images, and each sample was seen to be isotropic. The 2D images were then radially averaged to give the differential scattering cross section, after reduction to correct for detector efficiency and background scattering from the substrate.

In order to scale the SANS data to account for the varying thickness of films and quantify $I(Q)$ in units of cm^{-1}, image analysis was used to accurately determine the area of the irregularly shaped films so that thickness could be calculated from its mass and density. This is a more reliable approach than using calipers, which would be likely to damage the relatively soft film and yield low values for sample thickness. Images were captured using a diffuse light source and image analysis was subsequently performed using ImageJ.[22]

The SANS data with a single peak could be captured well by a broad peak model that can be used to identify the peak position and thus the distance between scattering inhomogeneities. In this model, the scattering intensity, $I(Q)$, is calculated as

https://dx.doi.org/10.1021/acs.langmuir.0c00084
Langmuir 2020, 36, 4795−4807

$$I(Q) = \frac{A}{q^n} + \frac{C}{1 + (|Q - Q_0|\xi)^m} + B \quad (1)$$

where A is the Porod law scale factor, n is the Porod exponent, C is the Lorentzian scale factor, m is the exponent of Q, ξ is the screening length, and B is the flat background. A limited range of the data containing a secondary peak at higher Q was also fitted with this simple model in order to extract the positions of the primary peak. Data was fitted to this model using the software Sasview.[21] Fitted parameters are included in the Supporting Information.

Dynamic Mechanical Analysis. Dynamic mechanical analysis was performed on samples in order to identify the glass transition temperatures. Samples for DMA were prepared by solution casting aqueous solutions of polymer and surfactant containing 10 wt % total solute. DMA was carried out with a temperature ramp from −40 to 100 °C at 3 °C min^{-1}, and subsequent cooling at the same rate, using a TA Instruments DMA Q800 system with nitrogen cooling. Samples were oscillated at a frequency of 1 Hz in an 8 mm 3-point bend geometry. The amplitude of the oscillation was set at 2% strain. The glass transition temperature was inferred from the maximum of the peak in tan δ, where δ is the phase angle, calculated as $\tan\delta = \frac{G''}{G'}$. An average value of the tan delta values determined upon heating and cooling the film was used.

RESULTS

Distribution of *N,N*-Dimethyldodecylamine *N*-Oxide in PVA films. Neutron reflectivity was used to determine the depth profiles of DDAO in spin-cast PVA films. The obtained reflectivity data could be fitted well to a three layer model, consisting of a thin surfactant-rich layer at the film−air interface, a bulk polymer-rich layer, and a layer of higher SLD corresponding to a silicon oxide layer on the substrate. For each composition profile presented, the numerical values for the layer composition, thickness, and roughness are tabulated and have been provided in the Supporting Information.

The observed SLD is made up of contributions from the two film components and is assumed to vary linearly with composition between the SLDs of pure PVA and pure dDDAO (eq 2) (any nonlinearity from a nonzero volume of mixing is likely to be negligible). The volume fraction profile of dDDAO, $\phi_{\mathrm{dDDAO}}(z)$, can therefore be determined from eq 3, where ρ is the measured SLD and ρ_{dDDAO} and ρ_{PVA} are the SLDs of pure dDDAO and pure PVA, respectively.

$$\rho(z) = \phi_{\mathrm{dDDAO}}(z)\rho_{\mathrm{dDDAO}} + \rho_{\mathrm{PVA}}(1 - \phi_{\mathrm{dDDAO}}(z)) \quad (2)$$

$$\phi_{\mathrm{dDDAO}}(z) = \frac{\rho - \rho_{\mathrm{PVA}}}{\rho_{dDDAO} - \rho_{\mathrm{PVA}}} \quad (3)$$

The depth profiles obtained from the binary films are shown as the solid lines in Figure 2. It should be noted that, due to limited available beam time, reflectivity for the film containing 2 wt % DDAO was collected using only the two smallest angles and is therefore missing the data at high Q. As a result, a slight increase in reflectivity can be identified at $Q \approx 0.2$ Å^{-1}, which would normally not be apparent upon stitching the data with that from the highest angle.

From these depth profiles, a very similar surface composition can be identified for each surfactant concentration. Values for the volume fraction ($\phi_{\mathrm{DDAO},1}$) and thickness (d_1) of the surfactant in the surface layer are equal in binary films with each surfactant loading, with the exception of the lowest loading of 2 wt % (Table 2). The thickness of surface layers of each film are consistent within the precision of the measurement (~5 Å), with the measured thickness corresponding well

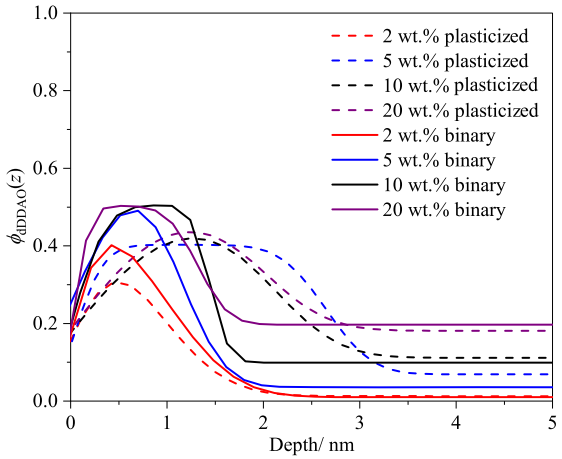

Figure 2. Volume fraction-depth profiles of 2−20% DDAO in binary and plasticized PVA films.

to a surfactant monolayer adsorbed onto the surface. The surface excess, z^*, defined by eq 4, where ϕ_b is the bulk additive concentration and $\phi(z)$ is the volume fraction profile in the surface region, was also calculated. This value can also be used to quantify additive segregation, as it represents the amount of material segregated from the bulk in excess of what the concentration would be if the bulk concentration persisted all the way to the interface. These values are also included in Table 2. In the binary films, little change in the surface excess with surfactant loading can be identified due to the large uncertainties associated with this measurement as a result of significant error propagation from each of the fitted parameters.

$$z^* = \int_0^\infty \phi(z) - \phi_b \, dz \quad (4)$$

NR was also used to explore the effect of the incorporation of glycerol as a model plasticizer on the distribution of deuterated DDAO in PVA films. The glycerol loading was fixed at 20 wt %, and the surfactant concentration was varied from 2 to 20 wt %. The volume fraction-depth profile of the deuterated surfactant was obtained by assuming an even distribution of glycerol throughout the film. These depth profiles are shown as the dashed lines in Figure 2.

For all surfactant loadings, the concentration of dDDAO in the surface layer is slightly reduced upon glycerol incorporation. Table 2 also includes the obtained values for the volume fractions of DDAO in the surface layer of plasticized films ($\phi_{\mathrm{DDAO},1}$) and the thickness of the surface layer, d_1. It can be seen that, as observed with the binary films, surfactant concentration and thickness of the surface layer is very similar for all surfactant loadings above 2 wt %, with both sets of values equal for each loading within the uncertainty of the fitted parameters. In the case of plasticized films, the consistent structure of the surface layer, regardless of the surfactant loading (with the exception of 2 wt %), results in a general decrease in the surface excess as the bulk surfactant concentration increases.

The depth profiles of samples containing deuterated surfactant appear to have a thicker silicon oxide layer adjacent to the substrate (up to 72 Å) than would be expected (approximately 25 Å, measured by ellipsometry for representative silicon blocks). This observation strongly suggests adsorption of the deuterated surfactant to the substrate

https://dx.doi.org/10.1021/acs.langmuir.0c00084
Langmuir 2020, 36, 4795−4807

Table 2. Thickness of Surface Layer (d_1), Surfactant Volume Fraction in the Surface Layer ($\phi_{DDAO,1}$), and Surface Excesses (z^*) of Binary and Plasticized Films Containing dDDAO

	$\phi_{DDAO,1}/10^{-2}$		d_1/nm		z^*/nm	
[dDDAO]/wt %	binary	plast.	binary	plast.	binary	plast.
2	50 ± 20	49 ± 6	1.0 ± 0.4	0.9 ± 0.1	0.4 ± 0.3	0.3 ± 0.1
5	60 ± 10	40 ± 3	1.1 ± 0.5	2.6 ± 0.3	0.5 ± 0.3	0.8 ± 0.2
10	60 ± 10	50 ± 10	1.4 ± 0.3	2.1 ± 0.4	0.5 ± 0.1	0.6 ± 0.2
20	56 ± 10	48 ± 3	1.2 ± 0.3	2.0 ± 0.2	0.5 ± 0.2	0.4 ± 0.1
40	54 ± 3		1.3 ± 0.2		0.24 ± 0.06	

interface. The SLD of the deuterated surfactant is similar to that of the silicon dioxide, and so adsorption of an additional surfactant layer would manifest itself in a thickening of the third layer in this three-layer model. To test this, reflectivity data for binary film containing 5 wt % dDDAO was fitted using a four-layer model, including an additional layer to account for surfactant absorption to the substrate interface. Although this does result in a slight improvement in the χ^2 values, the other fitted parameters (thickness and SLD of surface and bulk layers) are consistent within the uncertainty of these values. Due to the similar SLD of the enriched layer of deuterated surfactant and the silicon oxide, there is a great uncertainty in the thickness of this surfactant layer as these two components cannot be distinguished. Therefore, in order to avoid overparameterization, the reflectivity data for these systems is fitted using a three-layer model, although the thickness of the silicon oxide layer can reasonably be increased due to the presence of surfactant. The increase in thickness of the silicon oxide layer is of the order of that of a surfactant monolayer (≈20 Å). The similarity of the profiles obtained is demonstrated by the comparison of the fits and SLD profiles obtained using three- and four-layer models (Figure 3).

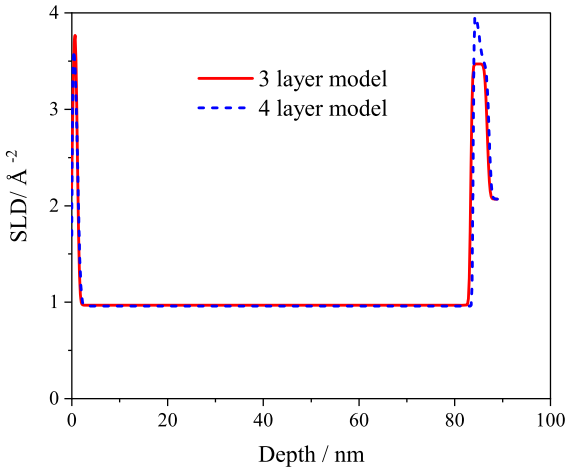

Figure 3. Neutron reflectivity data and fits for a film containing 5 wt % dDDAO fitted with a three-layer model and four-layer model (red and blue dashed lines, respectively).

Plasticizer Distribution in the Presence of Amine Oxide Surfactants. In order to identify any impact of amine oxide surfactants on the distribution of glycerol throughout the film, the SLD depth profiles of films consisting of PVA, deuterated glycerol, and hydrogenous DDAO were obtained. These are illustrated in Figure 4. There is much less contrast in SLD between PVA and the hydrogenous surfactants than between D-glycerol and the hydrogenous components, and so

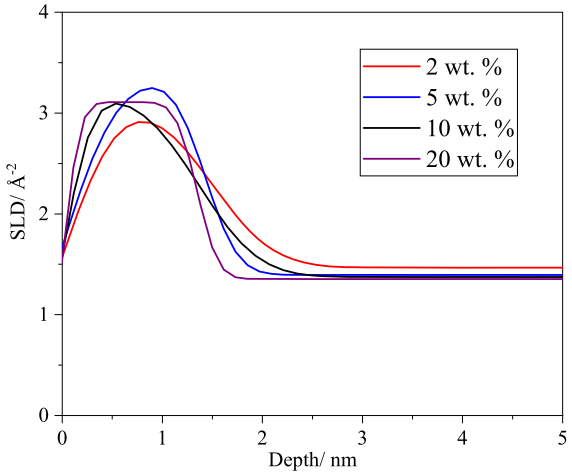

Figure 4. SLD depth profile obtained from reflectivity data for a film containing hDDAO from 2 to 20 wt % with 20 wt % D-glycerol.

the NR signal is almost entirely dominated by the depth distribution of the plasticizer.

Although the SLDs of the two hydrogenated components differ significantly, meaning eq 3 cannot be applied to accurately determine $\phi_{Gly}(z)$, the minimum and maximum concentration of glycerol on the surface can be determined by considering the remaining surface to be occupied fully by PVA and fully by hDDAO, which have SLDs of 0.75×10^{-6} and -0.20×10^{-6} Å^{-2}, respectively. The SLD of the surface layer in the presence of 5 wt % DDAO of 3.3×10^{-6} Å^{-2} corresponds to $0.61 \leq \phi_{Gly} \leq 0.69$.

This therefore reveals some segregation of the deuterated glycerol. Previous work has confirmed that no segregation of glycerol occurs in pure PVA/glycerol films.[17] The increased concentration of glycerol on the surface therefore reveals the coadsorption of DDAO and plasticizer into a monolayer on the film surface. Comparison of the SLD and thickness of this layer shows that, in the same manner as the surfactant distribution, the segregation of glycerol is consistent, regardless of the surfactant loading in the film, which further supports the hypothesis that z^* is independent of $\phi_{DDAO,tot}$. In contrast to the behavior of the surfactant, however, there was no evidence for glycerol enrichment at the substrate interface.

Impact of Surfactant Tail Length on Amine Oxide Distribution. The effect of the hydrophobicity of the surfactant on the segregation behavior was assessed by comparing the distribution of *N*,*N*-dimethyldodecylamine *N*-oxide with *N*,*N*-dimethyltetradecylamine *N*-oxide (DTAO) (12 and 14 carbons in the chain, respectively), in both binary and plasticized films. At a 20 wt % surfactant loading, DTAO exhibits very similar segregation behavior to DDAO, where a surfactant rich layer is present on the surface, the thickness of

https://dx.doi.org/10.1021/acs.langmuir.0c00084
Langmuir 2020, 36, 4795−4807

which corresponds well to a surfactant monolayer, with the remaining surfactant evenly distributed throughout the bulk of the film (Figure 5). As observed for DDAO, plasticization

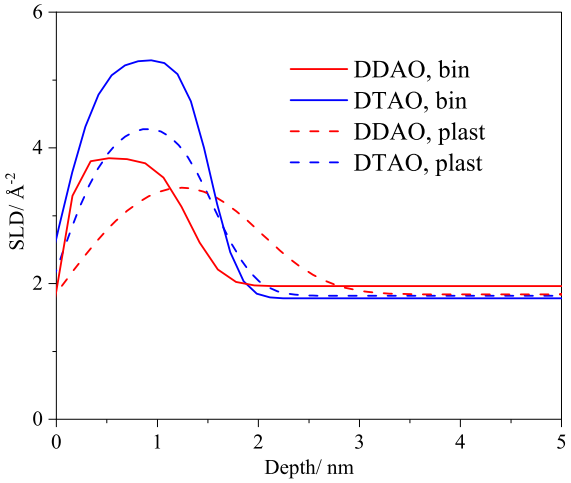

Figure 5. Comparison of the SLD depth profiles of PVA films containing dDDAO and dDTAO.

results in a decrease in the volume fraction of DTAO and increase in thickness of this layer, with no overall change in the surface excess. There is no measurable change in the thickness of the surface layer upon increasing the number of carbons in the alkyl chain from 12 to 14. However, there is a significant increase in the surfactant volume fraction in the surface layer and, as a result, a corresponding increase in the surface excess.

For both surfactants, the obtained depth profiles show behavior remarkably similar to that typically observed of surfactants in solution, with a monolayer adsorbed to the solution−air interface and the remaining present as aggregates in solution. Based on the assumption that this profile does indeed reflect an adsorbed pure monolayer on the surface, rather than a layer of PVA enriched in surfactant, it is possible to determine the area per molecule from the reflectivity fitted by modeling the adsorbed layer as a single uniform layer. The area per molecule, A, can be calculated using eq 5

$$A = \frac{\sum m_i b_i}{\rho \tau} \tag{5}$$

where ρ is the scattering length density, τ is the layer thickness, and $\Sigma m_i b_i$ is the total scattering length for the surfactant, with m_i being the number of atoms of scattering length b_i. The coherent scattering lengths of each isotope present in the surfactants are tabulated below (Table 3).

There are additional considerations in calculating the area per molecule in plasticized films. It is apparent from Figure 4 that glycerol is also enriched in the surface monolayer, coadsorbed with the surfactant, which will therefore have some contribution to the SLD of this layer. However, with the assumption that this surface monolayer in plasticized films contains only surfactant and glycerol, an approximation can be made. The SLD contribution from the hydrogenous component (glycerol) is calculated from the SLDs of the surface monolayer of the two contrasts via simultaneous equations and subtracted, to leave a corrected value for the SLD which arises solely from the deuterated component, and can be used to determine the area per molecule. Without making this correction in the SLD in order to account for the presence of glycerol in the surface layer, the calculated area per molecule is lower but generally within the uncertainty of the corrected value, demonstrating that the presence of the hydrogenated component has very little effect on the calculated value of area per molecule. The surfactant molecular areas in each of the films containing *N*,*N*-dimethyldodecylamine *N*-oxide (binary and plasticized) calculated using eq 5 are compared in Table 4.

Table 3. Coherent Scattering Lengths of Isotopes Present in the Surfactant Molecules Comprising the Surface Monolayer

atom	$b_i/10^{-5}$ Å
H	−3.74
D	6.67
C	6.65
N	9.36
O	5.80

Table 4. Area per dDDAO and dDTAO Molecule in the Surface Layer of Binary and Plasticized Films

	A/nm^2		
[dDDAO]/ wt %	binary	plasticized (uncorrected)	plasticized (corrected)
2	0.7 ± 0.3	0.8 ± 0.2	0.9 ± 0.2
5	0.5 ± 0.2	0.29 ± 0.06	0.35 ± 0.09
10	0.5 ± 0.1	0.33 ± 0.09	0.4 ± 0.1
20	0.5 ± 0.2	0.34 ± 0.05	0.40 ± 0.07
40	0.5 ± 0.1		
	A/nm^2		
[dDTAO]/ wt %	binary	plasticized (uncorrected)	plasticized (corrected)
20	0.36 ± 0.06	0.42 ± 0.05	

For DDAO, the area per molecule is unchanged with surfactant loading, suggesting that the structure of the monolayer is identical, irrespective of the total amount of surfactant present in the bulk of the film. For the plasticized films, the area per molecule is again unchanged with surfactant concentration, with the exception of the film with the 2 wt % loading, which is significantly larger. This suggests that there is less than full coverage at 2 wt % but above this the monolayer formed as a mixture of glycerol and surfactant is identical, regardless of the surfactant concentration. Due to the large uncertainties associated with the values for molecular area in the binary films, the effect of plasticization on the area per surfactant molecule on the surface monolayer is unclear, but appears to be small.

Film Surface Topography. Assessing the height maps of the film surface, and particularly considering the roughness of the film in conjunction with the measured depth profiles, can reveal information about the nature of the segregated layer, for example, highlighting the presence of defects. Height maps of representative regions of nonplasticized spin-cast films with areas of 2 μm^2 are shown in Figure 6. Although there is very little change in the surface upon increasing [DDAO] from 5 to 20 wt %, when [DDAO] is increased to 40 wt % the surface features become larger and more pronounced, although, as can be seen with the scale bar only ranging from −1 to 1 nm, the film is still very smooth.

https://dx.doi.org/10.1021/acs.langmuir.0c00084
Langmuir 2020, 36, 4795−4807

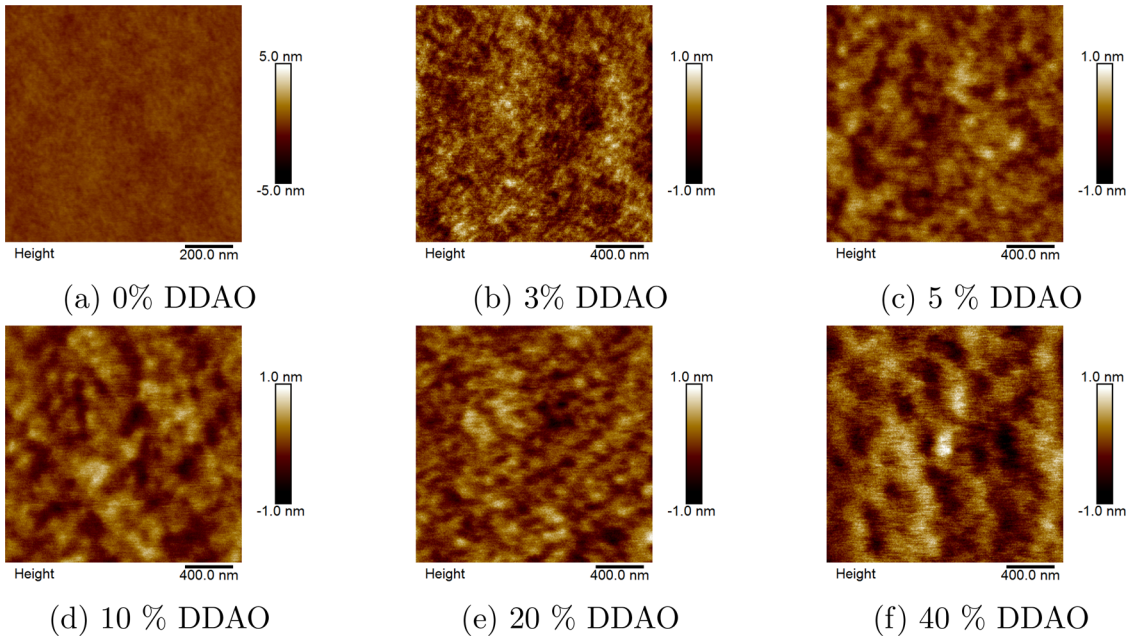

Figure 6. Height maps of nonplasticized PVA/DDAO films.

Figure 7 shows the change in root-mean-square roughness, R_q, and maximum height variation, R_{max}. There is no significant increase in R_q upon DDAO incorporation throughout the entire surfactant concentration range (even including the pure PVA film). Up to a concentration of 5 wt %, R_{max} also remains consistent with that of the pure PVA film. However, as the concentration is increased further, there is a substantial increase in R_{max} with [DDAO]. Despite this, the low and consistent values for average roughness shows that the surface monolayer, identified from the depth profiles obtained using neutron reflectivity, is very even across the surface. Roughness values are of the same order as measured by NR and tabulated in Supporting Information, although there is some variation between localized measurements on wafer-cast films (AFM) and large area averages blocks for NR.

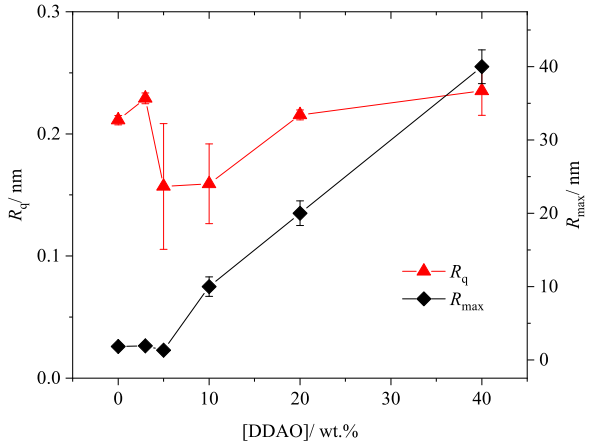

Figure 7. Change in root-mean-square roughness and maximum roughness of PVA films with DDAO loading.

Solution Properties of Amine Oxide Surfactants. The formation of monolayers rather than multilayer of these amine oxide surfactants in PVA films is different to that previously observed in any PVA/surfactant system.[16,17] However, this behavior is analogous to that of surfactants in solution. Surface tensiometry was used to characterize the behavior of the surfactants in water. Figure 8 shows that the surface tension of DDAO and DTAO solutions decrease to critical micelle concentrations of 0.024 and 0.0051 wt % respectively (1.1 and 0.20 mM). These values are similar to, but both slightly lower

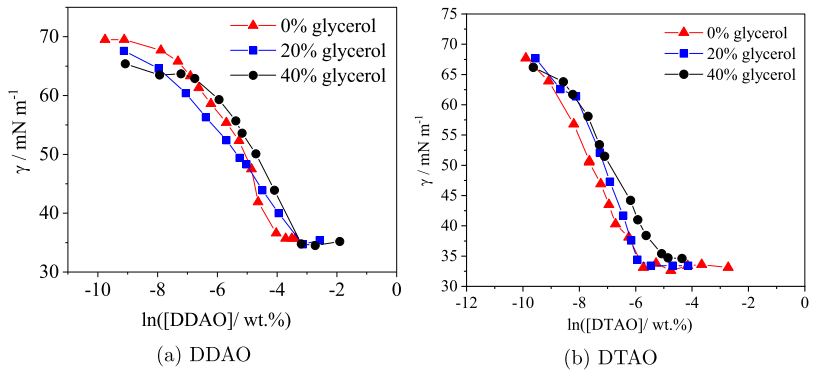

Figure 8. Surface tension of aqueous solutions of amine oxide surfactants in the presence of 0, 20, and 40% glycerol.

https://dx.doi.org/10.1021/acs.langmuir.0c00084
Langmuir 2020, 36, 4795−4807

Table 5. Comparison of Surface Excess (Γ) and Area Per Molecule of DDAO and DTAO in PVA Films and on the Water Surface

	DDAO			
	Γ/μmol m^{-2}		A/nm^2	
	solution	film	solution	film
binary	2.90 ± 0.09	3.3 ± 0.7*	0.57 ± 0.02	0.5 ± 0.2*
plasticized	4.89 ± 0.06	4.1−4.7*	0.58 ± 0.01	0.35−0.40*
	DTAO			
	Γ/μmol m^{-2}		A/nm^2	
	solution	film	solution	film
binary	4.9 ± 0.3	4.6 ± 0.5	0.34 ± 0.02	0.36 ± 0.04
plasticized	5.0 ± 0.1	4.0 ± 0.5*	0.33 ± 0.01	0.42 ± 0.05*

than those reported by Birnie et al.[23] (1.7 and 0.27 mM for DDAO and DTAO respectively).

The Gibbs adsorption equation, eq 6, enables the determination of the amounts of adsorbed surfactant from surface tension measurements.[24] Values for the surface excess, Γ, of the surfactant in solution are included in Table 5, where it can be seen that the values obtained in film and in solution are largely consistent. Comparison of the obtained area per molecule in solution, with the area per molecule on the polymer surface, determined from the fitted reflectivity data shows that DTAO occupies a smaller area per molecule than DDAO both in solution and in the film. Additionally, although there are fairly large uncertainties associated with the measurement of the area per molecule of DDAO, the areas per molecule on the film and solution surface are remarkably consistent for both surfactants studied.

The effect of plasticizer inclusion on the surface tension of solutions of the amine oxide surfactants is shown in Figure 8. The surface excesses of DDAO and DTAO were determined at glycerol concentrations of 0, 20, and 40 wt %. These values are included in Table 5 and illustrated in Figure 9 (values marked

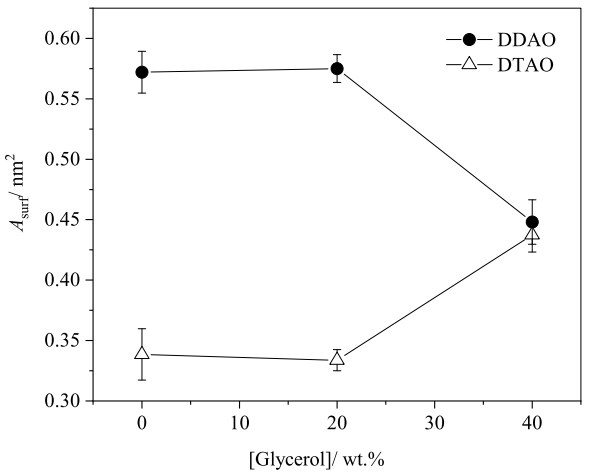

Figure 9. Change in molecular area of DDAO and DTAO on the solution surface with glycerol concentration

with an asterisk represented values that have not been corrected for the presence of hydrogenous glycerol in the surface layer). As previously stated, DTAO occupies a lower area per molecule than DDAO. As with the PVA matrix, addition of glycerol has relatively little impact on the surface excess. However, upon incorporation of 20 wt % glycerol the molecular area of both surfactants on the solution surface is unchanged. In contrast, at 40 wt % glycerol the two surfactants appear to converge to the same molecular area.

$$\Gamma = -\frac{1}{nRT}\left(\frac{d\gamma}{d\ln C}\right)_T \quad (6)$$

Compatibility of the PVA/Amine Oxide Surfactant System. Compatibility has been previously demonstrated to have a significant influence on surfactant segregation and the ternary phase diagrams have been shown to provide a useful measure of the compatibility of the PVA/water/SDS system.[16] PVA/water/amine oxide surfactant phase diagrams were constructed by determining points at which the system clouds during solution casting. The ternary phase diagrams for the PVA/DDAO/water and PVA/DTAO/water systems are shown in Figure 10. It can be seen that all compositions relevant for the formation of spin-cast films are well into the one-phase region; in the absence of water, over 50 wt % surfactant can be incorporated before phase separation occurs. There is surprisingly little difference in the phase behavior of DDAO and DTAO, which is reflected in their very similar depth profiles and segregation behavior. This shows that the significant increase in hydrophobicity with the extra $-C_2H_4$ group in DTAO is not obviously reflected by a change in compatibility with PVA. This result suggests that the unfavorable interaction between the surfactant tail group and the PVA matrix is less significant than it is in water, where the critical micelle concentration (CMC) is significantly dependent on the tail group length.

Small angle neutron scattering can provide further insight into the structures present in polymer samples, and thus be used as a tool to better understand the nature of the surfactant aggregates. Data was collected on PVA films containing amine oxides and/or glycerol in varying ratios.

SANS data for binary and plasticized films containing dDDAO and dDTAO at concentrations ranging from 0 to 40 wt % are shown in Figures 11 and 12, respectively. All samples scatter strongly, exhibiting a large peak in scattering intensity at $Q \approx 0.055$ Å^{-1}. Because the size of this peak increases with surfactant concentration, it strongly suggests the aggregation of the deuterated surfactant within the samples. However, the strong SANS signal and segregation of surfactant is not inconsistent with the apparent solubility of the surfactant from the phase diagrams. This is because light scattering/turbidity is on scale approaching microns at the least whereas SANS is sensitive to the smaller scale of semicrystalline domains.

https://dx.doi.org/10.1021/acs.langmuir.0c00084
Langmuir 2020, 36, 4795−4807

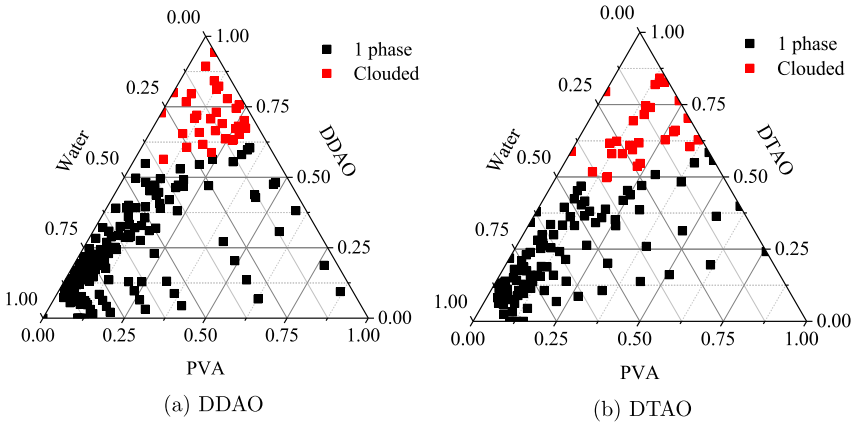

Figure 10. Ternary phase diagrams of the binary DDAO/PVA and DTAO/PVA systems, in units of mass fraction.

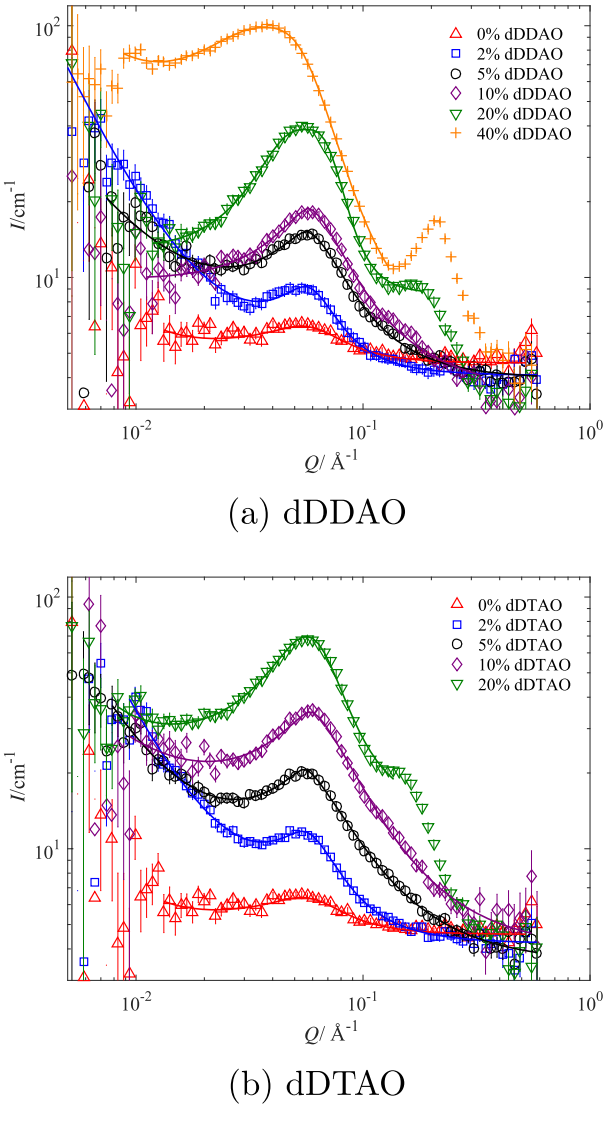

Figure 11. SANS data for the binary PVA/DDAO and PVA/DTAO systems. Solid curves are fits using the broad peak model.

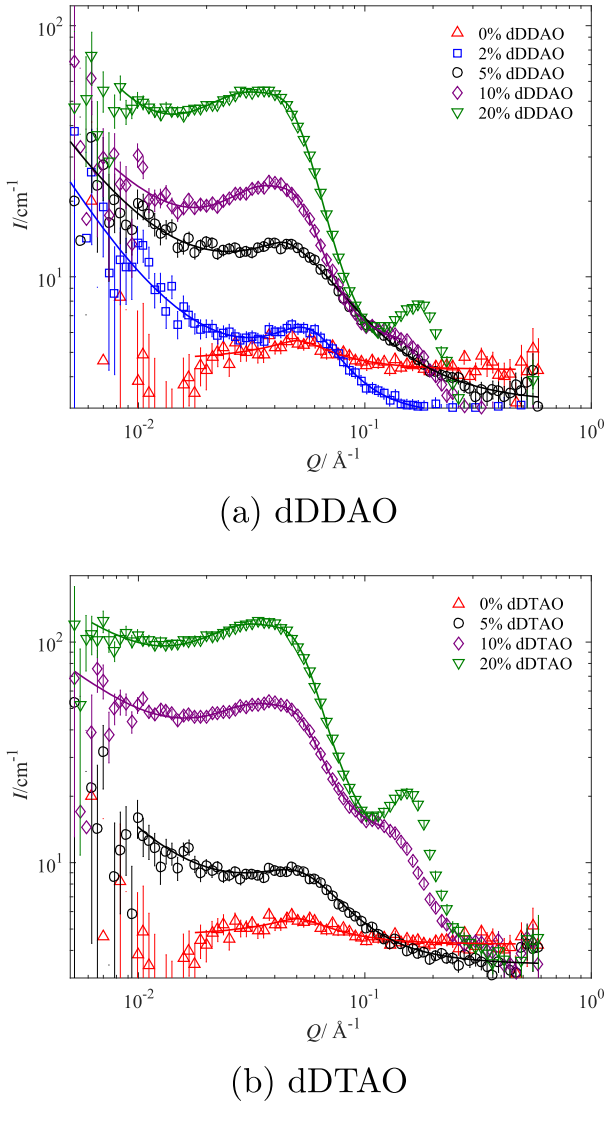

Figure 12. SANS data for the plasticized (20% glycerol) PVA/DDAO and PVA/DTAO systems. Solid curves are fits using the broad peak model.

The peak at $Q \approx 0.055$ Å^{-1} is present in all samples, including PVA in the absence of additional additives. This is therefore likely to be due to scattering from the interface between the amorphous and crystalline domains of the polymer, with contrast in the pure PVA arising due to the density differences of the two regions. The position of this peak in pure PVA ($Q_0 = 0.054$ Å^{-1}) is largely unchanged upon incorporation of either 20% D-glycerol or up to 20% deuterated amine oxide surfactants, strongly suggesting that scattering

https://dx.doi.org/10.1021/acs.langmuir.0c00084
Langmuir 2020, 36, 4795−4807

from the same structures is measured, but intensity is significantly greater in the latter system due to the increased contrast between amorphous and crystalline domains as a result of a higher concentration of additive with a greater SLD.

From the peak positions, determined from Q_0, the characteristic distance corresponding to this peak, d_0, can be calculated using eq 7. The variation in d_0 for binary and plasticized films containing dDDAO and dDTAO is shown in Figure 13.

$$Q = \frac{2\pi}{d} \tag{7}$$

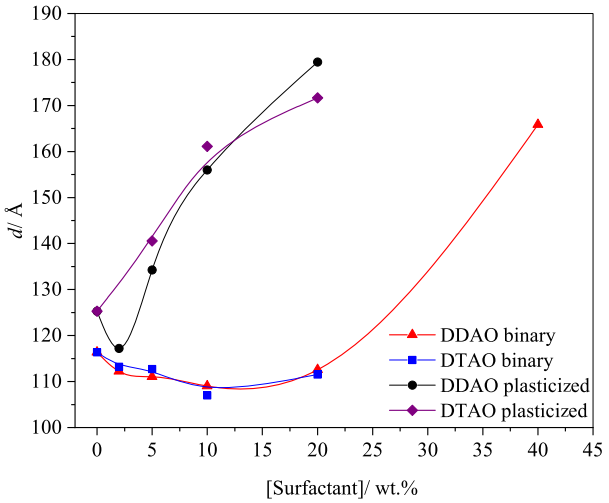

Figure 13. Spacing between scattering structures in binary and plasticized PVA films containing DDAO and DTAO, determined from peak positions of SANS data. Curves are a guide to the eye.

First considering the binary films, it can be seen that, in the concentration range of 2−20% surfactant, there is very little difference in the spacing between the regions occupied by DDAO and DTAO, and there is no significant change in d_0 with surfactant concentration. Upon incorporation of 40% DDAO, however, there is a substantial increase in d_0. There is no difference between the values for DDAO and DTAO, and thus this feature is not directly related to surfactant molecular structure.

In the case of the plasticized films, there is again very little difference between the spacing between scattering structures in PVA films containing DDAO and DTAO at each concentration. However, in contrast to the binary films, there is a general increase in d_0 with surfactant concentration.

At high surfactant loadings (20% DDAO and 10% DTAO) a secondary peak at higher Q appears (denoted Q_1). This is likely to be due to the structuring of the surfactant within the surfactant-rich domains, such as the formation of micelles. The position of this secondary peak is consistent with that previously observed for DDAO in solution, which has been consistently modeled as prolate ellipsoids.[25−27] The peak position is also related to the spacing, d, of the scattering inhomogeneities by eq 7. Based on $Q_1 \approx 0.15$ Å^{-1}, determined from the data corresponding to PVA containing 40% DDAO, the secondary peak corresponds to a distance, d_1, of 41 Å. This correlates well with the length of a fully extended DDAO bilayer.[28] Although a value for d_1 cannot be accurately determined from the SANS data on binary films, comparison of the secondary peak positions (Q_1) for DDAO and DTAO in plasticized PVA films reveals that Q_{1DDAO} (0.19 Å^{-1}) > Q_{1DTAO} (0.15 Å^{-1}), which reflects the larger size of the aggregates formed from the surfactant with the larger hydrocarbon tail.

DISCUSSION

Distribution of Components in PVA/Amine Oxide Surfactant Films. Neutron reflectivity has revealed that the amine oxide surfactants behave much like classical surfactants in PVA as well as water, forming a monolayer layer on the surface, but the majority of the surfactant is evenly distributed throughout the bulk film. In order to fairly compare the surfactant behavior in a range of model systems containing the different classes of surfactant, the same polymer used in previous systems, with a molecular weight range of 30−70 kg mol^{-1} and a degree of hydrolysis of 87−90%, was used to prepare the films. Although surfactant multilayer adsorption has been previously observed with $C_{12}E_5$[17] and SDS,[16] this is the first system where the adsorption is restricted to a single monolayer. Surface energy has been previously suggested to be largely responsible for segregation; comparison of the surface activity of the components in aqueous solution was able to rationalize the extensive segregation of SDS and $C_{12}E_5$ from PVA. Surface tensiometry has shown that the amine oxide surfactants have the lowest surface tension in solution of all components in the model film system. Therefore, based on our previous arguments, it would be favorable for them to segregate more extensively to the surface, with the amount of segregated additive dependent on the total amount of surfactant present. Despite this, very little surfactant is actually observed to segregate, and the amount of segregated surfactant is independent of the total amount present in the system. However, the substantially lower surface tension of DDAO and DTAO in solution compared to PVA is likely to lead to the formation of the surface monolayer in the solid films as this is sufficient to reduce the surface energy of the system.

We therefore also turn to compatibility arguments to rationalize the observed depth profiles, and postulate that most of the surfactant is present in the bulk film due to its high compatibility with the PVA matrix. Based on the minimal segregation observed even with very high surfactant concentration, it is probable that most of the surfactant is present in the bulk film due to its high solubility in the PVA matrix. This was confirmed by obtaining phase diagrams of the PVA/amine oxide/water systems, which reveal that a substantial amount of surfactant can be incorporated into the PVA matrix in the absence of water without phase separation occurring. Amine oxide surfactants are extremely hydrophilic, with their high hydrophilicity compared to other surfactants of the same chain length attributable to the strength of the dipole in the N−O bond of the amine oxide. This property could act to make them very compatible with the host polymer.[18] It is therefore likely that the strength of their interaction with hydroxyl groups in the PVA matrix can compensate for the free energy penalty of having the component with a lower surface free energy dispersed throughout the bulk.

The association of polymers and surfactants in solution to form polymer-bound micelles has been thoroughly documented, and it is well-established that nonionic and cationic micelles do not associate greatly with hydrophilic polymers.[29] Additionally, although Brackman and Engberts[30] reported the stabilization of micelles of DDAO in the cationic form by the hydrophobic polymers poly(vinyl methyl ether) and poly-

https://dx.doi.org/10.1021/acs.langmuir.0c00084
Langmuir 2020, 36, 4795−4807

(propylene oxide), no association between these polymers and the neutral form of DDAO was identified in solution. Association of neutral DDAO with polymers has been shown to occur only when the polymer is sufficiently hydrophobic.[29,31] Indeed DDAO showed no association with the relatively hydrophilic polymer poly(ethylene oxide). In the current work with PVA, with the solutions at the natural pH, the surfactants are almost exclusively in the neutral form and therefore little interaction with the hydrophilic PVA in solution would be expected. However, this does not preclude the possibility of the amine oxide surfactants interacting favorably with hydroxyl groups present in amorphous regions of the solid film matrix.

Influence of Plasticizer on Surface Properties of Three-Component Films. The replacement of some PVA with glycerol on the depth profile of surfactants in PVA films can have a significant impact of surfactant and plasticizer distribution due to the competing compatibilities of the three components. However, we surprisingly observe very little difference in the segregation of the amine oxide upon glycerol incorporation other than a slight thickening of this layer, and an increased area per surfactant molecule for DDAO. The adsorption of glycerol onto the surface over a similar length scale to the thickness of the adsorbed surfactant layer signifies the coadsorption of this species with the surfactant into a more diffuse monolayer, but no other surface enrichment. It was previously noted that the incorporation of glycerol into a film containing CTAB results in the segregation of the surfactant that was not observed in the binary film which is suggested to result from glycerol out-competing CTAB for sites in the amorphous regions of the matrix.[17] It was also shown that glycerol enables the formation of thermodynamically stable stacked SDS/glycerol layers on the film surface, allowing even more SDS to segregate than was observed in binary films. In the current system, the depth profiles observed therefore suggests a greater compatibility of the amine oxide with the matrix, even in the presence of plasticizer, probably due to the hydrophilicity of the surfactant.

Interfacial Adsorption. The thick region of high SLD ($\sim 3.8 \times 10^{-6}$ Å^{-2}) on the substrate interface apparent in the SLD depth profiles of films containing deuterated surfactant (Figure 3) is strongly indicative of interfacial surfactant adsorption. Although neutron reflectivity is not capable of resolving the nature of the structures at the interface of these films spun onto a silicon substrate due to the similar SLD of the silicon oxide and the PVA containing this volume fraction of deuterated surfactant, there has been substantial evidence for the formation of structures on solution-substrate interfaces. When reflectivity data for a PVA/DDAO film was fitted with a 4-layer model, to include an additional surfactant-rich layer adjacent to the substrate, the thickness of the interfacial layer was found to be 13 ± 10 Å, which could correspond to a number of different structures, which have been probed theoretically and experimentally.[32−35] The significant uncertainty in this value is a result of the difficulty in resolving the interfacial surfactant from the SiO_x (25 ± 15 Å). It was previously reported that treating structured surfactant films as a bilayer generally results in a good fit to reflectivity data.[35] This surfactant rich layer present adjacent to the silicon substrate could therefore correspond either to a monolayer, as observed on the surface, a bilayer-type structure consisting of a surfactant head group closest to the hydrophilic substrate, a tail region, and another head group region adjacent to the bulk polymer film, or a more complex structure such as cylindrical aggregates, as observed in the case of nonionic DTAO on the mica-solution interface by Kawasaki et al.[36] The evidence from NR suggests that, similarly to the behavior observed in solution, structures are forming on the film−substrate interface. They are not multilayered, however, and are therefore consistent with the single-phase behavior of the surfactant in the bulk. Although here we do not focus on the nature of these aggregates, this finding presents convincing evidence that the behavior of the surfactant in the solid film is parallel to that in solution.

Structure of Surface Monolayer: DDAO vs DTAO in Film and Solution. It is particularly noteworthy that the surfactant exhibits identical behavior when water is replaced by a solid polymer, given the significant differences in surface tension of pure water and pure PVA. Although a range of surface energy values for PVA have been reported, from 37 to 59 mN m^{-1}[37−39] depending on the degree of hydrolysis and molecular weight, all are higher than the surface tension of the surfactant solutions above the CMC. This strongly suggests that difference in surface energy is not the predominant driving force for this segregation, as concluded in previous systems.

When discussing the nature of the surfactant behavior both in the film and in solution, it is important to acknowledge the equilibrium between the protonated and unprotonated forms of the surfactant. The equilibrium constant, K_a is defined as

$$K_a = \frac{[(CH_3)_2RNO^-][H^+]}{[(CH_3)_2RNOH]} \tag{8}$$

The pK_a can be written in terms of the degree of ionization of the micelle, α_M

$$pK_a = pH + \log[\alpha_M/(1 - \alpha_M)] \tag{9}$$

At neutral pH, the amine oxides are almost exclusively in the neutral form, although the presence of the cationic species should be considered. The pK_m value can be defined as the intrinsic proton dissociation constant of the micelle, rather than the single surfactant molecules. This is known to be greater than that of the single surfactant molecule.[40,41] It is particularly relevant that Maeda and Kakehashi[18] have shown that DDAO and DTAO have significantly different pK_m values. Despite having identical head group chemistry, the interfacial arrangement, which is partly governed by the size of the tail groups, has an impact on the head group separation and so the degree of dissociation. As a result, p$K_{m(DDAO)}$ (5.89) is smaller than p$K_{m(DTAO)}$ (6.30), meaning that a higher concentration of the cationic species of DTAO is likely to be present in solution than in the corresponding DDAO solution. This is thought to be a result of the different shapes of the largely nonionic micelles; DDAO has been shown to form spherical micelles, whereas DTAO forms rodlike micelles. Although these pK_m values were taken in solutions containing 1 M NaCl, it was determined that the salt concentration has no significant effect on pK_m. The degree of protonation therefore affects both the solution and surface properties of the surfactant, including CMC, aggregation number, and aggregate shape. This is due to the well-known hydrogen bonding between cationic and nonionic amine oxide groups,[42] the likely formation of hydrogen bonds between two neighboring cationic groups,[43] and the dipole−dipole interactions between the nonionic species.[18] Solutions for both surface tension measurements and spin-casting were used at natural pH, above pH 7, and the

https://dx.doi.org/10.1021/acs.langmuir.0c00084
Langmuir 2020, 36, 4795−4807

amine oxide groups in these conditions are predominantly nonionic.

However, analysis of the Gibbs isotherms has shown that DTAO occupies a significantly smaller area per molecule than DDAO does. As the area per molecule on the surface is highly sensitive to the degree of ionization (α) of the surfactants, it is probable that the lower area per molecule is due to the slightly greater degree of ionization of DTAO (although a substantially greater degree of ionization would lead to a greater molecular area due to greater head group repulsion). However, the dissociation constants of the surfactant monomers are not identical to that in the micelle as the introduction of charges is generally more favored on the micelle surface. Despite this, it is plausible that even a slightly higher concentration of the cationic surfactant in DTAO solutions would result in the formation of strong hydrogen bonds on the surface between the cationic and nonionic head groups, leading to the formation of dimers and decreasing the average area per head group. This effect is then replicated in the solid film, where the area per molecule is greater for DDAO than DTAO, with values consistent with those of the area on the solution surface. This suggests that the nature of interactions is consistent when the bulk is water or solid PVA.

Influence of Glycerol on Surfactant Molecular Area. At the highest concentration, the presence of glycerol has the opposite effect on the areas of the DDAO and DTAO molecules both in the film and solution. With a pK_a of 14.4,[44] the incorporation of glycerol into the mixtures is expected to have a negligible increase in the proportion of the cationic species from that of the binary solutions. We therefore suggest that it is the interaction between the surfactant head groups and the plasticizer molecules that affects the area per molecule on the surface. This should be addressed by considering the nature of the interactions between the surfactant and glycerol.

The effect of glycerol on surfactant behavior has been addressed in a number of systems including ionic and nonionic surfactants,[45−47] although there have been no reported studies on the effect of cosolutes such as glycerol on the surface tension or micellization behavior of amine oxide surfactants. In general two different mechanisms for the action of cosolvents such as glycerol on the micellization of surfactants have been suggested. The first is an indirect mechanism, where the additive changes the properties of the aqueous medium, in particular the dielectric constant, which impacts the electrostatic interaction in solution. This is generally accepted in the case of ionic surfactants. The second is a direct mechanism, where the additive replaces some of the water molecules that hydrate the surfactant. D'Errico et al.[45] investigated the effects of glycerol on the cationic surfactant CTAB and the nonionic ethoxylated surfactant Brij 58. Although the CMC of CTAB is affected by the presence of the cosolute only above 30 wt % glycerol, above this concentration the area per surfactant molecule was found to increase almost linearly with the glycerol concentration. The average area per Brij 58 molecule on the surface was also found to follow a generally linear increase with concentration. In both of these systems, the authors found no evidence of a direct interaction between the surfactant and glycerol molecules. However, different behavior could be reasonably expected of the amine oxide surfactants studied in this work due to the strong N−O dipole and ability to form strong hydrogen bonds with the additive.

It is surprising that, in solutions containing 40 wt % glycerol, the molecular areas of DDAO and DTAO appear to be equal, given that this suggests a decrease in molecular area for the former surfactant and increase in molecular area for the latter. This is likely to be a result of the breakdown in ideality assumed in determining the molecular area using the Gibbs Adsorption equation. It is possible that this nonideality is caused by the hydrogen bonding between glycerol and amine-oxide groups, rather than the presence of any cationic-nonionic hydrogen bonds. It is plausible that the strength of hydrogen bonds between glycerol and the surfactant head group are stronger than the dipole−dipole interactions between the nonionic head groups predominantly present in the DDAO solution/film.

The lack of change of molecular area in solution for both surfactants when glycerol content is increased from 0 to 20 wt % is surprising. This behavior suggests that in this system, the monolayer is unaffected by the cosolute at this loading as there is no coadsorption of glycerol in solution. (This is in contrast to the solid film, where enrichment of D-glycerol to the surface of PVA containing 20 wt % D-glycerol is apparent, Figure 4). This argument can be used to explain the observations in both solution and films. However, the inconsistency of the values for A_{surf} between solution and film in the presence of 20 wt % glycerol suggests a subtle difference in the behavior of surfactants when water is replaced by a solid polymer; in the presence of the PVA, much lower loading of glycerol is required for its coadsorption to the surface.

Compatibility of the PVA/Amine Oxide Surfactant System. The high compatibility of the PVA/amine oxide surfactant system, as revealed by the ternary phase diagram, was previously discussed in terms of its role in the resulting surfactant distribution in spin-cast films. This high compatibility of the amine oxides with PVA can also be corroborated with findings from small angle neutron scattering. First, SANS demonstrates that these molecules are localized in specific regions already present in the polymer. As it is clear from the SANS data that the surfactants localize in the same region as glycerol, a commonly used plasticizer, it is probable that DDAO and DTAO are localized in the amorphous regions of the polymer. This was confirmed by the effect of DDAO on the glass transition temperature of PVA films was measured using DMA (presented in the Supporting Information). If the additive localizes in the amorphous regions, a change in glass transition temperature would result, whereas this would not be expected should the additive localize exclusively in the crystalline regions, or as a separate phase. From the clear decrease in T_g with DDAO concentration it can be concluded that the amine oxides occupy the amorphous regions, contributing to the plasticization of the PVA.

The lack of change in d_0 upon increasing the concentration of both DDAO and DTAO from 0 to 20% (Figure 11) suggests that these additives can be incorporated at a high loading without substantially changing the overall structure of the polymer. With 40% DDAO, however, the size of the amorphous domains must increase to accommodate the surfactant, leading to an increase in d_0. In contrast to the binary films, in plasticized films, where 20% glycerol is additionally incorporated, the inclusion of as little as 5% surfactant causes a substantial increase in d_0, which increases almost linearly with additive concentration. This likely indicates that the preferential occupation of both surfactant and plasticizer in the amorphous domains causes an increase in size of these regions and a resulting greater spacing between the crystallites.

https://dx.doi.org/10.1021/acs.langmuir.0c00084
Langmuir 2020, 36, 4795−4807

CONCLUSION

Two zwitterionic surfactants have shown segregation behavior in PVA remarkably similar to their behavior in water, showing molecular areas that are equal in solution and in the film. Neutron reflectivity has additionally shown that the composition of the surface of the films is the same, regardless of the surfactant loading. To date, this is the only polymer/surfactant system observed where the surfactant has such similar behavior to that in aqueous solution. This has been attributed to the small amine-oxide group which affords the surfactant a high level of compatibility with the polymer matrix. The head group is also capable of strong dipole−dipole bonds with adjacent head groups, resulting in the favorable formation of a monolayer on the surface. Comparison of the molecular area of DDAO and DTAO shows that the longer chain surfactant has a lower molecular area, which is due to the higher degree of ionization and hence the stronger interhead group interactions. The nature of the intermolecular interactions in the monolayer can be used to justify the effect of the incorporation of glycerol on the molecular areas of DDAO. Although there are some subtle differences between the surfactant behavior in solution and in the film, the remarkable and unprecedented similarity between the systems demonstrates the importance of the interactions between the head groups. Furthermore, these surfactants, which are unusually compatible with PVA, were also observed to have a distinct plasticizing effect on the polymer matrix, which may be a significant consideration for using PVA films to encapsulate surfactants and their mixtures.

ASSOCIATED CONTENT

Supporting Information

The Supporting Information is available free of charge at https://pubs.acs.org/doi/10.1021/acs.langmuir.0c00084.

Fitting parameters from SANS and NR experiments, and plot of glass transition temperature against DDAO concentration in solution cast PVA films (PDF)

AUTHOR INFORMATION

Corresponding Author

Richard L. Thompson − *Department of Chemistry, Durham University, Durham DH1 3LE, United Kingdom;* orcid.org/0000-0002-3207-1036; Email: r.l.thompson@durham.ac.uk

Authors

Rebecca J. Fong − *Department of Chemistry, Durham University, Durham DH1 3LE, United Kingdom; Procter & Gamble, Newcastle Innovation Centre, Newcastle-upon-Tyne NE12 9TS, United Kingdom;* orcid.org/0000-0003-2389-7140

Ophélie Squillace − *Department of Chemistry, Durham University, Durham DH1 3LE, United Kingdom; School of Chemical Engineering, University of Birmingham, Birmingham B15 2TT, United Kingdom*

Carl D. Reynolds − *Department of Chemistry, Durham University, Durham DH1 3LE, United Kingdom; School of Chemistry, University of Birmingham, Birmingham B15 2TT, United Kingdom*

Joshaniel F. K. Cooper − *Rutherford Appleton Laboratories, Didcot OX11 0QX, United Kingdom*

Robert M. Dalgliesh − *ISIS Neutron and Muon Source, Rutherford Appleton Laboratories, Didcot OX11 0QX, United Kingdom;* orcid.org/0000-0002-6814-679X

James Tellam − *Rutherford Appleton Laboratories, Didcot OX11 0QX, United Kingdom*

Florence Courchay − *Procter & Gamble, Brussels Innovation Center, 1853 Brussels, Belgium*

Complete contact information is available at: https://pubs.acs.org/10.1021/acs.langmuir.0c00084

Notes

The authors declare no competing financial interest.

ACKNOWLEDGMENTS

The authors thank EPSRC/Procter and Gamble (UK) and the Soft Matter and Functional Interfaces CDT (SOFI-CDT) for supporting this work via EP/L015536/1 and to STFC for provision of the neutron reflection and SANS facilities through beamtime allocations https://doi.org/10.5286/ISIS.E.RB1720329 and https://doi.org/10.5286/ISIS.E.RB1720244). This work benefited from the use of the SasView application, originally developed under NSF Award DMR-0520547. SasView contains code developed with funding from the European Union's Horizon 2020 research and innovation programme under the SINE2020 project, Grant Agreement No. 654000.

REFERENCES

(1) Aramendia, E.; Mallégol, J.; Jeynes, C.; Barandiaran, M. J.; Keddie, J. L.; Asua, J. M. Distribution of Surfactants near Acrylic Latex Film Surfaces: A Comparison of Conventional and Reactive Surfactants (Surfmers). *Langmuir* **2003**, *19*, 3212−3221.

(2) Zhao, C. L.; Holl, Y.; Pith, T.; Lambla, M. FTIR-ATR spectroscopic determination of the distribution of surfactants in latex films. *Colloid Polym. Sci.* **1987**, *265*, 823−829.

(3) Evanson, K. W.; Thorstenson, T. A.; Urban, M. W. Surface and interfacial FTIR spectroscopic studies of latexes. II. Surfactant-copolymer compatibility and mobility of surfactants. *J. Appl. Polym. Sci.* **1991**, *42*, 2297−2307.

(4) Du Chesne, A.; Gerharz, B.; Lieser, G. The Segregation of Surfactant upon Film Formation of Latex Dispersions: an Investigation by Energy Filtering Transmission Electron Microscopy. *Polym. Int.* **1997**, *43*, 187−196.

(5) Gundabala, V. R.; Zimmerman, W. B.; Routh, A. F. A Model for Surfactant Distribution in Latex Coatings. *Langmuir* **2004**, *20*, 8721−8727.

(6) Lee, W. P.; Gundabala, V. R.; Akpa, B. S.; Johns, M. L.; Jeynes, C.; Routh, A. F. Distribution of Surfactants in Latex Films: A Rutherford Backscattering Study. *Langmuir* **2006**, *22*, 5314−5320.

(7) Xu, G. H.; Dong, J.; Severtson, S. J.; Houtman, C. J.; Gwin, L. E. Modifications of Surfactant Distributions and Surface Morphologies in Latex Films Due to Moisture Exposure. *J. Phys. Chem. B* **2009**, *113*, 10189−10195.

(8) Arnold, C.; Thalmann, F.; Marques, C.; Marie, P.; Holl, Y. Surfactant Distribution in Waterborne Acrylic Films. 1. Bulk Investigation. *J. Phys. Chem. B* **2010**, *114*, 9135−9147.

(9) Zhang, J.; Severtson, S. J.; Houtman, C. J. Characterizing the Distribution of Sodium Alkyl Sulfate Surfactant Homologues in Water-Based, Acrylic Pressure-Sensitive Adhesive Films. *J. Phys. Chem. B* **2011**, *115*, 8138−8144.

(10) Gromer, A.; Thalmann, F.; Hébraud, P.; Holl, Y. Simulation of Vertical Surfactant Distributions in Drying Latex Films. *Langmuir* **2017**, *33*, 561−572.

(11) Ben Halima, N. Poly(vinyl alcohol): review of its promising applications and insights into biodegradation. *RSC Adv.* **2016**, *6*, 39823−39832.

(12) Lim, M.; Kim, D.; Seo, J. Enhanced oxygen-barrier and water-resistance properties of poly(vinyl alcohol) blended with poly(acrylic acid) for packaging applications. *Polym. Int.* **2016**, *65*, 400−406.
(13) Matsumura, S.; Shimura, Y.; Terayama, K.; Kiyohara, T. Effects of molecular weight and stereoregularity on biodegradation of poly(vinyl alcohol) byAlcaligenes faecalis. *Biotechnol. Lett.* **1994**, *16*, 1205−1210.
(14) Matsumura, S.; Kurita, H.; Shimokobe, H. Anaerobic biodegradability of polyvinyl alcohol. *Biotechnol. Lett.* **1993**, *15*, 749−754.
(15) Mohsin, M.; Hossin, A.; Haik, Y. Thermal and mechanical properties of poly(vinyl alcohol) plasticized with glycerol. *J. Appl. Polym. Sci.* **2011**, *122*, 3102−3109.
(16) Briddick, A.; Fong, R. J.; Sabattié, E. F. D.; Li, P.; Skoda, M. W. A.; Courchay, F.; Thompson, R. L. Blooming of Smectic Surfactant/Plasticizer Layers on Spin-Cast Poly(vinyl alcohol) Films. *Langmuir* **2018**, *34*, 1410−1418.
(17) Briddick, A.; Li, P. X.; Hughes, A.; Courchay, F.; Martinez, A.; Thompson, R. L. Surfactant and Plasticizer Segregation in Thin Poly(vinyl alcohol) Films. *Langmuir* **2016**, *32*, 864−872.
(18) Maeda, H.; Kakehashi, R. Effects of protonation on the thermodynamic properties of alkyl dimethylamine oxides. *Adv. Colloid Interface Sci.* **2000**, *88*, 275−293.
(19) Singh, S. K.; Bajpai, M.; Tyagi, V. K. Amine Oxides: A Review. *J. Oleo Sci.* **2006**, *55*, 99−119.
(20) Nelson, A. Co-refinement of multiple-contrast neutron/X-ray reflectivity data using *MOTOFIT*. *J. Appl. Crystallogr.* **2006**, *39*, 273−276.
(21) Doucet, M. et al. *SasView*, version 4.2, 2018; http://www.sasview.org/.
(22) Schneider, C. A.; Rasband, W. S.; Eliceiri, K. W. NIH Image to ImageJ: 25 years of image analysis. *Nat. Methods* **2012**, *9*, 671−675.
(23) Birnie, C. R.; Malamud, D.; Schnaare, R. L. Antimicrobial evaluation of N-alkyl betaines and N-alkyl-N, N-dimethylamine oxides with variations in chain length. *Antimicrob. Agents Chemother.* **2000**, *44*, 2514−7.
(24) Ikeda, S.; Tsunoda, M.-A.; Maeda, H. The application of the Gibbs adsorption isotherm to aqueous solutions of a nonionic-cationic surfactant. *J. Colloid Interface Sci.* **1978**, *67*, 336−348.
(25) Barlow, D. J.; Lawrence, M. J.; Zuberi, T.; Zuberi, S.; Heenan, R. K. Small-Angle Neutron-Scattering Studies on the Nature of the Incorporation of Polar Oils into Aggregates of N,N-Dimethyldodecylamine-N-oxide. *Langmuir* **2000**, *16*, 10398−10403.
(26) Warisnoicharoen, W.; Lansley, A. B.; Lawrence, M. J. Nonionic oil-in-water microemulsions: the effect of oil type on phase behaviour. *Int. J. Pharm.* **2000**, *198*, 7−27.
(27) Lorenz, C. D.; Hsieh, C.-M.; Dreiss, C. A.; Lawrence, M. J. Molecular Dynamics Simulations of the Interfacial and Structural Properties of Dimethyldodecylamine-N-Oxide Micelles. *Langmuir* **2011**, *27*, 546−553.
(28) Baglioni, M.; Benavides, Y. J.; Berti, D.; Giorgi, R.; Keiderling, U.; Baglioni, P. An amine-oxide surfactant-based microemulsion for the cleaning of works of art. *J. Colloid Interface Sci.* **2015**, *440*, 204−210.
(29) Ruckenstein, E.; Huber, G.; Hoffmann, H. Surfactant aggregation in the presence of polymers. *Langmuir* **1987**, *3*, 382−387.
(30) Brackman, J. C.; Engberts, J. B. F. N. Effect of Surfactant Charge on Polymer-Micelle Interactions: N-Dodecyldimethylamine Oxide. *Langmuir* **1992**, *8*, 424−428.
(31) Goddard, E. Polymer-Surfactant Interaction Part I. Uncharged Water-Soluble Polymers and Charged Surfactants. *Colloids Surf.* **1986**, *19*, 255−300.
(32) Poptoshev, E.; Claesson, P. M. Adsorption of dimethyldodecylamine-N-oxide at the mica-solution interface studied by ellipsometry. *Colloids Surf., A* **2006**, *291*, 45−50.
(33) Ngo, D.; Baldelli, S. Adsorption of Dimethyldodecylamine Oxide and Its Mixtures with Triton X-100 at the Hydrophilic Silica/Water Interface Studied Using Total Internal Reflection Raman Spectroscopy. *J. Phys. Chem. B* **2016**, *120*, 12346−12357.
(34) Tiberg, F.; Landgren, M. Characterization of thin nonionic surfactant films at the silica/water interface by means of ellipsometry. *Langmuir* **1993**, *9*, 927−932.
(35) Schulz, J. C.; Warr, G. G.; Hamilton, W. A.; Butler, P. D. A New Model for Neutron Reflectometry of Adsorbed Surfactant Aggregates. *J. Phys. Chem. B* **1999**, *103*, 11057−11063.
(36) Kawasaki, H.; Syuto, M.; Maeda, H. Effects of Protonation on the Aggregate Structures of Tetradecyldimethylamine Oxide at Solid Solution Interfaces. *Langmuir* **2001**, *17*, 8210−8216.
(37) Lee, L.-H. Relationships between surface wettability and glass temperatures of high polymers. *J. Appl. Polym. Sci.* **1968**, *12*, 719−730.
(38) van Oss, C.; Chaudhury, M.; Good, R. Monopolar surfaces. *Adv. Colloid Interface Sci.* **1987**, *28*, 35−64.
(39) Wu, S. Estimation of the critical surface tension for polymers from molecular constitution by a modified Hildebrand-Scott equation. *J. Phys. Chem.* **1968**, *72*, 3332−3334.
(40) Tokiwa, F.; Ohki, K. Potentiometric Titration of a Nonionic-Cationic Surfactant in Aqueous Solution. *J. Phys. Chem.* **1966**, *70*, 3437−3441.
(41) Maeda, H.; Tsunoda, M.; Ikeda, S. Electric and nonelectric interactions of a nonionic-cationic micelle. *J. Phys. Chem.* **1974**, *78*, 1086−1090.
(42) Maeda, H. Dodecyldimethylamine oxide micelles: stability, aggregation number and titration properties. *Colloids Surf., A* **1996**, *109*, 263−271.
(43) Maeda, H.; Muroi, S.; Kakehashi, R. Effects of Ionic Strength on the Critical Micelle Concentration and the Surface Excess of Dodecyldimethylamine Oxide. *J. Phys. Chem. B* **1997**, *101*, 7378−7382.
(44) Serjeant, E. P.; Dempsey, B. In *Ionisation Constants of Organic Acids in Aqueous Solution. International Union of Pure and Applied Chemistry (IUPAC). IUPAC Chemical Data Series No. 23*; Serjeant, E. P., Dempsey, B., Eds.; Permagon: Oxford, 1979; p 384.
(45) D'Errico, G.; Ciccarelli, D.; Ortona, O. Effect of glycerol on micelle formation by ionic and nonionic surfactants at 25 C. *J. Colloid Interface Sci.* **2005**, *286*, 747−754.
(46) Hamel, A.; Sacco, M.; Mnasri, N.; Lamaty, F.; Martinez, J.; De Angelis, F.; Colacino, E.; Charnay, C. Micelles into Glycerol Solvent: Overcoming Side Reactions of Glycerol. *ACS Sustainable Chem. Eng.* **2014**, *2*, 1353−1358.
(47) Sarkar, B.; Lam, S.; Alexandridis, P. Micellization of Alkyl Propoxy Ethoxylate Surfactants in Water Polar Organic Solvent Mixtures. *Langmuir* **2010**, *26*, 10532−10540.

https://dx.doi.org/10.1021/acs.langmuir.0c00084
Langmuir 2020, 36, 4795−4807